Electrical Power and Energy Systems 55 (2014) 312–320

Contents lists available at ScienceDirect

Electrical Power and Energy Systems

journal homepage: www.elsevier.com/locate/ijepes

Optimal power flow of a wind-thermal generation system

Yu-Cheng Chang [a], Tsung-Ying Lee [a,*], Chun-Lung Chen [b], Rong-Mow Jan [a]

[a] Department of Electrical Engineering, Ming Hsing University of Science and Technology, Taiwan, ROC
[b] Department of Marine Engineering, National Taiwan Ocean University, Taiwan, ROC

ARTICLE INFO

Article history:
Received 9 October 2012
Received in revised form 4 February 2013
Accepted 25 September 2013

Keywords:
Wind generation system
Optimal power flow
Spinning reserve
Particle swarm optimization

ABSTRACT

Many expect wind energy to continue increasing due to falling capital costs, market scalability, and its low environmental impact. As more wind turbine generators are connected to utility systems, it is becoming more important to study the impact of wind turbine generators (WTGs) on power system operations. Wind generation system will affect not only the economic operation of a power system but also the bus voltage and transmission losses due to different locations of wind generation system. Optimal power flow (OPF) program is a useful tool for power system operation and planning. This study proposes an Evolutionary Particle Swarm Optimization (EPSO) approach for the optimal power flow problem. The proposed model considers up-spinning reserves, down-spinning reserves and the operational constraints of the generation unit. The effects of wind generation on power system operation and planning are investigated. This study uses the load and unit data of a modified IEEE 30 bus power system to test the corrective of the new method. The OPF results in this study satisfy the operational requirements of a wind-thermal power system. This study also applies the developed OPF program to estimate the effects of wind generation on power system operation and the planning. Experiment results show that the developed OPF program is a useful tool for wind-thermal power system operation and the planning. The results of this study can serve as a reference for wind-thermal power system operation and the planning.

1. Introduction

As more wind turbine generators are connected to utility systems, it is becoming more important to study the impact of wind turbine generators (WTGs) on system operations. A power system with wind turbine generators (WTGs) must consider two spinning reserves in the generation scheduling problem. The up spinning reserve (USR) is the reserve capacity for a sudden load increase, unpredictable fall in wind turbine generator power output, or forced outage of thermal generators. It is closely related to, and nearly proportional to, the output of the wind generation system (WGS). The down spinning reserve (DSR) is the reserve capacity designed for sudden load decreases and unpredictable increases in wind turbine generator power output. It is designed to compensate for possible fluctuation in wind generation system power output. The thermal generation units might turn on and turn off frequently if the down reserve is not considered in the power system operation.

Wind generation system will affect not only the economic operation of a power system but also the bus voltage and transmission losses due to different locations of wind generation system. For the reason of maintaining the energy efficiency of power system operation, both the effects of wind generation on power system economic operations and the effects of wind generation on bus voltage and transmission losses should be studied. Optimal power flow (OPF) is one of the most important topics in power system operations that including economic operation and power flow analysis.

An optimal power flow (OPF) solution adjusts the network settings of a power system to achieve objective functions and meet the requirements of equipment operation constraints, power flow equations, and power system security. The objective function of an OPF program is to minimize the fuel costs of a power system. Thus, the solution parameters include the real power output of generators, transformer taps, and capacitor bank taps. OPF is a complex problem that includes economic dispatch and power flow solutions[1–4]. Researchers have developed many mathematical methods for OPF solving, including linear programming, sequential quadratic programming, the generalized reduced gradient method, and the Newton method. These methods are good in convergence, and many power companies use them. However, these mathematical methods also have several drawbacks: (1) the objective functions and constraints must be continuity, convexity, and differentiability; (2) the chances of falling into a local optimum are high; (3)

* Corresponding author. Address: 1, Hsin-Hsing Road, Hsin-Feng, Hsin-Chu, Taiwan, ROC.
E-mail address: tylee@must.edu.tw (T.-Y. Lee).

0142-0615/$ - see front matter © 2013 Elsevier Ltd. All rights reserved.
http://dx.doi.org/10.1016/j.ijepes.2013.09.028

changing the objective functions and constraints requires large changes [5].

Recently, with the emergence of artificial and computational intelligence technologies, such as neural network, genetic algorithm, and evolutionary programming, have also been applied to deal with the OPF problem. The authors of [6] describe an initialization procedure in solving optimal power flow by genetic algorithm (GA). Simulation results show that the proposed initialization procedure improves the performance of the whole GA-OPF procedure. Another study [7] presents a hybrid neural-network and genetic algorithm (GAANN) technical for solving OPF with voltage security constraint. Artificial neural networks are employed to learn in an offline mode. Genetic algorithm (GA) is employed as the optimization tool. Simulation results indicate that the proposed GAANN is capable of performing OPF calculation with much less time and the results are quite accurate comparing to the conventional GA-OPF method. The authors of [8] formulated transient stability-constrained into optimal power flow problem. Other studies [9–14] developed a novel PSO approach to solve an optimal power flow problem with embedded security constraints and transient stability constraints. Case studies show that PSO is useful as an alternative to solve the challenging OPF problem. Another study [15] proposed an efficient parallel GA for the solution of large-scale OPF with consideration of practical generators constraints. Results show that the proposed method is able to provide satisfactory performance, and obtains the solution with high accuracy. The authors of [16] reported a multi-objective harmony search algorithm for optimal power flow problem. Computational results indicate that the proposed method is not only able to ensure the operating constraints of the system, but also determine a lower fuel cost solution compared with other reported results in the literature. The authors of [17] describe a modified honey bee mating optimization to solve Dynamic optimal power flow. In [18], a new evolutionary optimization algorithm for optimal power flow in a power system involving unified power flow controller is proposed. The authors of [19] reported a hybrid particle swarm optimization and simulated annealing for Dynamic optimal power flow solution. A new hybrid algorithm for optimal power flow considering prohibited zones and valve point effect is reported in [20]. The authors of [21] describe a modified shuffle frog leaping algorithm for multi-objective optimal power flow solving. Although the features of these approaches are quite different, they were proposed in order to either decrease the computation time or to reduce the fuel costs of power systems. Few publications focus on the effects of up/down spinning reserves on the OPF of a wind-thermal power system, or the affects of a wind generation system on power system OPF operations. Further, the literature rarely discusses the problem of how to solve the OPF problem for a wind-thermal power system.

This study addresses the following research gaps:

1. Is it possible to solve the OPF problem for a wind-thermal power system?
2. What are the effects of a wind generation system on power system spinning reserve requirements and abilities?
3. What are the effects of a wind generation system on power system economic dispatch operations?
4. How does wind turbine location affect the bus voltage, transmission loss, and fuel costs of a power system?

This paper is organized as follows. Section 2 details the problem formulation and the objective function. Section 3 describes the wind generation model. The development and working of the EPSO approach is elaborated in Section 4. Section 5 discusses simulation and experimental results made on a standard test system. Finally, Section 6 concludes the paper.

2. Problem formulation and the objective function

The OPF problem is a complex problem that includes economic dispatch and power flow solutions. The objective function of an OPF program is to minimize the fuel costs of a power system. The solution parameters include the real power output of generators, transformer taps, and capacitor bank taps. The OPF problem in this paper includes wind generation units and up/down spinning reserves. The objective function of this problem is expressed as follows:

$$\textit{Minimize} \quad F_t = \sum_{i=1}^{N} F_i(P_{Gi}) \tag{1}$$

where F_t is total fuel cost; P_{Gi} is generation of thermal unit i; N is number of on-line thermal units. The control variables of Eq. (1) are generation of thermal units, bus voltages of voltage-controlled buses, transformer tap and reactive power injection of shunt capacitors. In this paper, we assume the wind turbine generators have no cost in the OPF problem.

The OPF problem has two categories of constraints:

(1) *Equality constraints:* These are the sets of nonlinear equations that govern the power system, i.e.,

(a) Real power balanced

$$\sum_{i=1}^{N} P_{Gi} + P_{WT} - P_{loss} - P_D = 0 \tag{2}$$

$$P_{loss} = \sum_{J=1}^{BL} G_J[|V_x|^2 + |V_y|^2 - 2|V_x||V_y|\cos(\delta_x - \delta_y)] \tag{3}$$

where P_{WT} is summation of power output of all WTGs; P_D is the total load; P_{loss} is transmission loss; BL is number of transmission lines; G_J is conductance of the line between buses x and y; $|V_x|$ is voltage magnitude of bus x; δ_x is voltage angle of bus x.

(b) Power flow equations

$$P_i - \sum_{k=1}^{BN} |V_i V_k Y_{ik}| \cos(\theta_{ik} - \delta_i + \delta_k) = 0 \tag{4}$$

$$Q_i + \sum_{k=1}^{BN} |V_i V_k Y_{ik}| \sin(\theta_{ik} - \delta_i + \delta_k) = 0 \tag{5}$$

where P_i and Q_i are real and reactive power injected into power system at bus i; BN is the number of buses; Y_{ik} is the element in the ith row and kth column of bus admittance matrix; θ_{ik} is angle of the element in the ith row and kth column of bus admittance matrix.

(2) *Inequality constraints*

These are the set of discrete and continuous constraints that represent the system security and operational limits as the following:

(a) Bus voltage limits

$$V_i^{min} \leqslant V_i \leqslant V_i^{max}, \quad i = 1, 2, \ldots, BN \tag{6}$$

where $V_i^{\min}$ is lower voltage limit of bus i; $V_i^{\max}$ is upper voltage limit of bus i; BN is number of buses.

(b) Transformer tap setting limits

$$TP_s^{min} \leqslant TP_s \leqslant TP_s^{max}, \quad s = 1, 2, \ldots, TN \tag{7}$$

where TP_s^{min} is lower tap limit of transformer s; TP_s is tap of transformer s; TP_s^{max} is upper tap limit of transformer s; TN is number of transformer.

(c) Reactive power tap setting of capacitors

$$QC_h^{min} \leqslant QC_h \leqslant QC_h^{max}, \quad h = 1, 2, \ldots, CN \tag{8}$$

where QC_h^{min} is lower tap limit of capacitor h; QC_h is tap of capacitor h; QC_h^{max} is upper tap limit of capacitor h; CN is number of capacitor. The capacitors are modeled as reactive power injection in the OPF problem.

(d) Transmission limit of lines

$$SL_l \leqslant SL_l^{max}, \quad l = 1, 2, \ldots, BL \tag{9}$$

where SL_l is line flow of line l; SL_l^{max} is line flow limit of line l; BL is number of lines.

(e) Power limits of generation unit

$$Q_{Gi}^{min} \leqslant Q_{Gi} \leqslant Q_{Gi}^{max}, \quad i = 1, 2, \ldots, N \tag{10}$$

$$P_{Gi}^{min} \leqslant P_{Gi} \leqslant P_{Gi}^{max}, \quad i = 1, 2, \ldots, N \tag{11}$$

where P_{Gi}^{min} is minimum real power limit of thermal unit i; P_{Gi}^{max} is maximum real power limit of thermal unit i; Q_{Gi}^{min} is minimum reactive power limit of thermal unit i; Q_{Gi}^{max} is maximum reactive power limit of thermal unit i.

(f) Spinning reserve constraints

$$\sum_{i=1}^{N} US_i \geqslant P_D \times s\% + P_{WT} \times r\% \tag{12}$$

$$\sum_{i=1}^{N} DS_i \geqslant P_{WT} \times r\% \tag{13}$$

where US_i is the maximum USR limit of thermal unit i; $s\%$ is percentage of load contributing to up spinning reserve; $r\%$ is percentage of wind generation contributing to USR and DSR; DS_i is the maximum DSR limit of thermal unit i.

Constraints (2)–(11) can be considered by solving the power flow problem at each time stage. Constraints (12), (13) will be handled during the process of EPSO.

3. Wind generation model

The power output of a WTG can be determined using the functional relationship between the wind speed and the power output of the WTG as (14). Fig. 1 shows a typical power curve for a WTG. Region UD to UF is nearly a 3rd order polynomial. The power output of a WTG is approximated by a 3-order polynomial as (14).

$$P_w(U_u) \begin{cases} P_w^r, & UX > U_u \geqslant UF \\ b \cdot U_u^3 + c \cdot U_u^2 + d \cdot U_u + e, & UF > U_u > UD \\ 0, & U_u \leqslant UD \\ 0, & U_u \geqslant UX \end{cases} \tag{14}$$

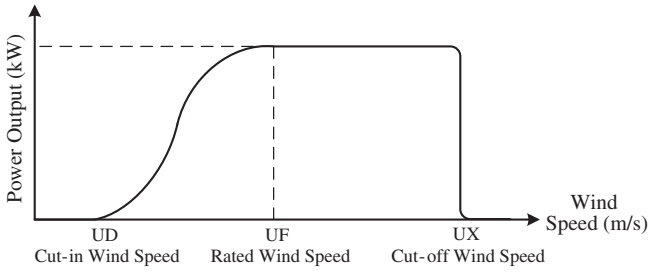

Fig. 1. A typical power curve for a WTG.

$P_w(U_u)$ is the available WTG power output. The parameters used are the wind speed at hub height U_u, the WTG rated wind speed UF, the WTG cut-in wind speed UD and the WTG cut-off wind speed UX. The parameters b, c, d and e are constants.

The model in this study assumes that the power factor of wind turbine generators is 1.0, and uses the generation output of wind turbine generators as a negative real power load, connected to a special bus, in power flow study.

The effect of uncertainty of wind turbine generators is an important issue in wind generation researches. A computer program named "HOMER" was applied to generate hourly wind speed data from the recorded long-term wind speed data at the test site [22]. This program generated the wind speed probability by a Weibull probability density function. Wind speed uncertainty was considered in this program.

4. Overall approach

Particle swarm optimization (PSO) is an efficient approach for solving nonlinear optimization problems. It is originally mimics the sociality of bird block and fish school. Through a tracking of two best values, i.e., *Pbest* and *Gbest*, the global optimum might be achieved by this optimization technique [23]. The main drawback of PSO is that it easily gets trapped in a local optimal solution. Evolutionary programming (EP) is a parallel search algorithm [24]. It is a global search algorithm with the ability to reach a global or near global optimal solution. However, EP has lower computational efficiency than PSO.

Evolutional Particle Swarm Optimization (EPSO) [25] incorporates PSO with EP to enhance the computation efficiency of EP and enable PSO to jump out of the local optimum. The mutation and competition mechanisms of EP enable EPSO to jump out of the local optimum. The velocity and position updating mechanisms of PSO enhance the computation efficiency of EPSO. This paper proposes an EPSO approach for solving the OPF problem of a wind-thermal power system. The overall approach involves the following steps:

Step 1: Read system data and setup parameters.
Step 2: Generate initial solutions.
Step 3: Use a fast-decoupled power flow program to compute the generation of the independent thermal unit and check the operational constraints of the power system.
Step 4: Calculate the fitness of every solution.
Step 5: Generate offspring population.
Step 6: Check the boundary limits.
Step 7: Check the end conditions. If the end conditions are satisfied, go to step 7, otherwise, go to step 3.
Step 8: Print out the results.

The following subsections describe this procedure in detail.

4.1. Define the elements of an individual

An individual is a solution in EPSO. Each individual is a $[DM \times 1]$ matrix, and its elements include the real power output of $N-1$ thermal units, the bus voltage of BX voltage controlled buses, transformer tap of TN transformers, and reactive power injection of CN shunt capacitors. DM is the summation of $(N-1)$, BX, TN, and CN. N is the number of thermal units, BX is the number of voltage-controlled buses, TN is the number of transformers, and CN is the number of shunt capacitors. The tap position of transformer is a discrete variable with a discrete step size of 0.01 in this paper.

4.2. Generate the initial population randomly

EPSO is a parallel search approach. Many individuals cooperate to find the global optimum. The process begins with a randomly generated initial population, and ends when the difference between all individuals are sufficiently small. A good initial solution enhances the possibility of obtaining an optimal solution. The computation steps to generate elements in an individual within the initial population are as follows:

Step 1: Randomly generate the generation of thermal units, within the feasible region shown in (11), and meet the up/down spinning reserve constraints shown in (12), (13)
Step 2: Randomly generate the bus voltages of voltage-controlled buses, within the bus voltage limits in (6).
Step 3: Randomly generate the transformer tap, within the transformer tap setting limits in (7). Round the tap to the nearest discrete transformer tap position.
Step 4: Randomly generate the reactive power injection of shunt capacitors, within the reactive power tap setting of capacitors in (8).
Step 5: Repeats Steps 1–4 for J times to build an initial population, which includes J individuals. J is the population size.

The initial solutions are generated within their feasible region, thus the constraints are satisfied.

4.3. Perform power flow analysis

Use a fast-decoupled power flow program to compute the power flow solutions of every individual. This step also calculates the generation of the independent thermal unit, and checks the power system operation constraints illustrated in (2), (3), (4), (5), (6), (9), and (10).

4.4. Evaluate the fitness of each individual

Calculate the value of each individual's fitness function. The fitness function, shown in Eq. (1), is an index that evaluates the fitness of an individual. This study uses the generation of the independent thermal units, solved in Section 4.3, and generation of other thermal units, to compute the fitness of each individual.

4.5. Generate the offspring population

EPSO is a hybrid algorithm, which is a combination of Evolutionary Programming and particle swarm optimization. The procedure to generate an offspring population in EPSO is as follows:

Step 1: Generate offspring of individuals by EP mutation. An offspring is created around a parent by adding a Guassian random variable to the parent. This step generates the offspring of individuals x_j^k for $j = 1, 2, 3, \ldots, J$ by EP mutation. Eq. (15) shows the mutation mechanism. Where, x_j^k is individual j in iteration k, $x_j^{k'}$ is offspring of individual j in iteration k, σ_j is range of offspring created around the parent j, $N_j(0,1)$ is a Gaussian random variable with mean 0 and standard deviation 1 that is regenerated for every individual j.

$$x_{j+J}^{k'} = x_j^k + \sigma_j N_j(0,1) \tag{15}$$

Step 2: Competition and selection by EP. An EP competition mechanism is applied to select better individuals. Each individual in the combined population of that generated in step 1, and the parents, must compete with M number of individuals, randomly chosen from the combined population. M is number of competitors. Every individual will obtain a competition score. Compare the competition score of the parent and its offspring. The winner becomes the offspring.
Step 3: Update velocity and position of the first J individuals obtained in step 2, using PSO updating rules. The velocity and position updating rules of PSO are applied to further modify the individuals obtained in step 2. The velocity of a particle represents a movement of the elements shown in Section 4.1. The position of a particle is the value of elements. The updated individuals form the next generation. This step updates the positions of x_j^k for $j = 1, 2, 3, \ldots, J$ to be the offspring of the next generation. Where, $x_j^{k'}$ is offspring of individual j in iteration k. Eqs. (16) and (17) are applied to update the *Pbest* and *Gbest* in the searching process. *Pbest* is the best value of fitness function of every individual it has been achieved, *Gbest* is the best value of fitness function that has been achieved so far by any individual. If the current solutions of them are better than the latest values, then replace them by the best value in the current iteration. *Pbest* and *Gbest* contain the same elements as an individual.

$$\begin{aligned} Gbest^k &= X_{A1}^{B1},\ FT\left(X_{A1}^{B1}\right) \\ &= \min\cdot\left\{FT\left(X_{C1}^{D1}\right),\ C1 \in [1,J],\ D1 \in [1,k]\right\} \end{aligned} \tag{16}$$

$$\begin{aligned} Pbest_j^k &= X_{A3}^{B3},\ FT\left(X_{A3}^{B3}\right) \\ &= \min\left\{FT\left(X_{C3}^{D3}\right),\ C3 = j,\ D3 \in [1,k]\right\} \end{aligned} \tag{17}$$

where $FT(\cdot)$ is fitness function, $Gbest^k$ is *Gbest* from beginning to iteration k, $Pbest_j^k$ is the *Pbest* of individual j from beginning to iteration k. Eq. (18) is applied to update the velocity of individuals.

$$\begin{aligned} V_j^{k+1} &= w \cdot V_j^k + c1 \cdot rand\left(Pbest_j^k - X_j^k\right) + c2 \\ &\quad \cdot rand\left(Gbest^k - X_j^k\right) \end{aligned} \tag{18}$$

Eq. (19) is applied to update the position of individuals.

$$X_j^{k'} = X_j^k + V_j^{k+1} \tag{19}$$

4.6. Check the boundary limits

There are different ways to handle constraints in evolutionary computation optimization algorithms. In this paper, a preserving feasible solution method is applied. Solutions are initially placed in the feasible search space and remain within by adapting an update mechanism that generates only feasible solutions. If any element of an individual breaks its inequality constraints then the position of the individual is fixed to its maximum/minimum operating point.

4.7. Check the end condition

If the end condition is reached, the algorithm stops, otherwise, increase iteration number, and repeat the steps stated in Section 4.3–4.5. In this study, EPSO will stop if one of the following criteria is satisfied: (1) The best fitness between two consecutive iterations is unchanged for 10 iterations, (2) the variation of the best fitness is within a permit range, and (3) the maximum number of iterations (*ITmax*) is reached.

5. Numerical examples

The following examples illustrate the OPF problem of a wind-thermal power system. Consider a modified IEEE 30 bus test system [5]. This system includes 6 generators, 41 transmission lines, 2 shunt capacitors, 4 tap-changing transformers, and 20 loads. Two capacitors banks installed at buses 5 and 24 have ratings of 19 and 4 MVAR, respectively. The base value is 100 MVA. Bus 1 is the slack bus. The real power load is 189.2 MW, and the reactive power load is 107.2 MVAR. This set-up ignores emission data. Fig. 2 shows a single-line diagram of the test system, and Table 1 shows the parameters of the generation system. The ramp up/down rates are 20–30% of the maximum power output. P_{Gi}^{0} represents the generator power output at the first hour.

The simulated wind generation system connects to a special bus in the modified IEEE 30 bus system. This study includes four case studies. First, Section 5.1 demonstrates the effectiveness of applying the EPSO approach to the OPF problem. Then, Sections 5.2–5.4 analyzes the effects of wind generation on power system OPF operations. The parameters $c1$, $c2$, w and σ of the EPSO algorithm were tuned according to experiment results and experiences.

5.1. OPF analysis of the modified IEEE 30 bus power system

This study uses the proposed OPF computer program to compute the OPF solution of the modified IEEE 30 bus power system. Two case studies demonstrate the effectiveness of the proposed OPF computer program. In the first case, transformer taps and shunt capacitors remain constant. The total real power generation is 191.605 MW, the total operating cost is 574.766 $/h, and the total transmission loss is 2.408 MW. All operational constraints are satisfied.

In the second case, the operating range of four tap-changing transformers is between 0.9 and 1.05, with a discrete step size of 0.01. The capacitor banks at buses 5 and 24 are control variables with a range of 0 MVAR to 40 MVAR and a step size of 1 MVAR [5]. The OPF program adjusts the transformer taps and shunt capacitors during the computation procedure. The resulting total real power generation is 191.433 MW, with a total operating cost of 573.928 $/h and a total transmission loss of 2.233 MW.

Table 2 shows the computation results, and compares the results of case 1 and case 2. This table shows that the transmission loses and the total operating costs of case 2 are less than that in case 1. These results show that the proposed OPF program can not only calculate the real power output of generators that

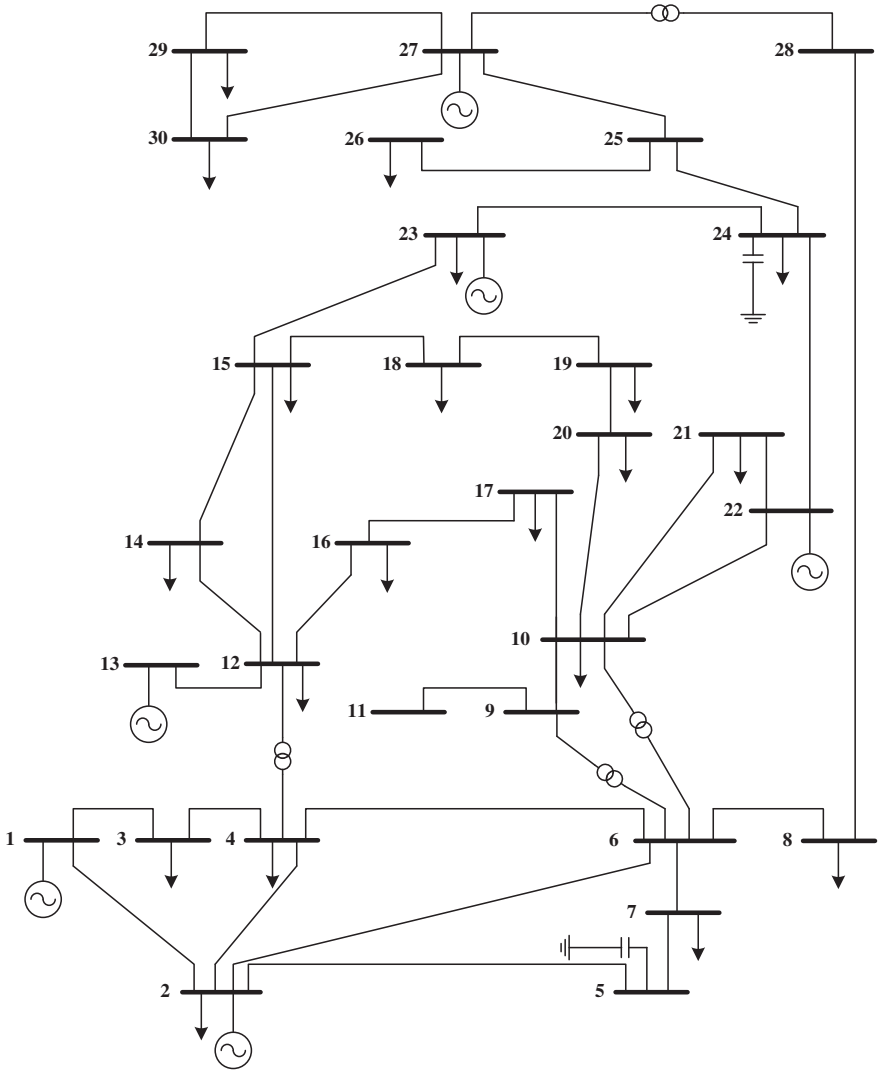

Fig. 2. Single-line diagram of the modified IEEE 30-bus test system.

Table 1
Generation unit characteristics.

Generator no.	Bus no.	$P_{Gi,\min}$ (MW)	$P_{Gi,\max}$ (MW)	$Q_{Gi,\min}$ (MVar)	$Q_{Gi,\max}$ (MVar)	UR_i (MW/h)	DR_i (MW/h)	P_{Gi}^0 (MW)
1	1	0	80	−20	150	20	20	40
2	2	0	80	−20	60	20	20	60
3	13	0	40	−15	44.7	10	10	20
4	22	0	50	−15	62.5	10	10	20
5	23	0	30	−10	40	10	10	15
6	27	0	55	−15	48.7	10	10	40

Table 2
The best OPF solution of the modified IEEE 30-bus test system.

	Case 1	Case 2
P_{g1}	43.425	43.535
P_{g2}	55.785	57.220
P_{g13}	17.716	18.066
P_{g22}	23.131	22.559
P_{g23}	18.241	17.569
P_{g27}	33.307	32.482
V_1	1	1.014
V_2	0.999	1.088
V_{13}	1.061	1.100
V_{22}	1.071	1.086
V_{23}	1.076	1.092
V_{27}	1.1	1.100
Q_{c5}	–	7
Q_{c24}	–	14
T_{6-9}	–	1.01
T_{6-10}	–	0.96
T_{4-12}	–	0.98
T_{27-28}	–	1.04
Total generation (MW)	191.605	191.433
Total fuel cost ($/h)	574.766	573.928
Transmission loss (MW)	2.408	2.233

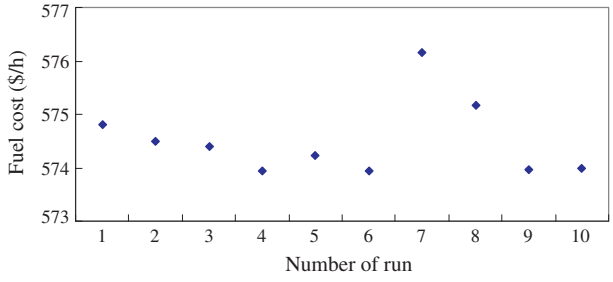

Fig. 3. Distribution of total fuel cost of case 2.

achieves a minimum total fuel cost, but also can automatically adjust the transformer taps and shunt capacitors to achieve the minimum transmission losses.

To demonstrate the effectiveness and consistency of the proposed OPF program, 10 independent runs were performed for case 2 to determine EPSO's ability to reach an optimal or near-optimal solution. Fig. 3 shows the distribution of total fuel cost of the results obtained by the proposed EPSO approach for 10 different runs. Table 3 is statistical data for case 2. The largest total fuel cost is 576.151 $/h, the best total fuel cost is 573.928 $/h, the average total fuel cost is 574.505 $/h, the standard deviation of total fuel cost is 0.711 $/h. The results in Table 3 and Fig. 3 demonstrate the good performance of EPSO in solving the OPF problem.

The results of implementing OPF over a modified IEEE 30-bus test system using the proposed EPSO approach along with the other methods are presented in Table 4. Results clearly indicate that EPSO achieved better solution in both cases.

Table 3
Statistical data for case 2.

	Worst	Best	Mean	Standard deviation
Total generation (MW)	191.788	191.433	191.551	0.115
Transmission loss (MW)	2.588	2.233	2.401	0.120
Total fuel cost ($/h)	576.151	573.928	574.505	0.711

Table 4
Results of the minimum cost compared with different methods.

	Case 1			Case 2		
	Total generation (MW)	Loss (MW)	Cost ($/h)	Total generation (MW)	Loss (MW)	Cost ($/h)
SQP [5]	192.060	2.860	576.892	–	–	–
PSO	191.847	2.647	575.411	191.769	2.569	575.244
HPSO [5]	191.847	2.647	575.411	191.455	2.255	574.143
EPSO	191.605	2.408	574.766	191.433	2.233	573.928

5.2. Effects of wind generation on power system operating costs and spinning reserves

This study evaluates the effects of wind generation on power system operating costs and spinning reserves. Wind generation systems with capacities of 10% (Scenario 1), 20% (Scenario 2) and 30% (Scenario 3) of the power system load were connected to bus 8, respectively. The wind speed of the 1st hour was assumed to be 3 m/s. Tables 5–7 calculate and list the operating costs and spinning reserve of the 2nd hour, under different wind speeds.

In this test, the spinning reserve is 15% of the total load, i.e., $s\%$ = 15%. An extra spinning reserve is set to improve power system safety operation under uncertain wind generation conditions. The extra spinning reserve is 50% of wind generation, i.e., $r\%$ = 50%.

Table 5 shows the computation results of Scenario 1. The wind speed of the 2nd hour varies from 4 m/s to 11 m/s. This table also shows the spinning reserve requirements and spinning reserve abilities of the power system, as well as operating costs. The generation of the wind generation system increases as the wind speed increases. Meanwhile the total operating costs decrease as the wind speed increases. In this case, the up/down spinning reserve capacity of the power system, supplied by thermal generators, is greater than the up/down spinning reserve requirement for all wind speed conditions.

Table 6 shows the computation results of Scenario 2. In this case, when the wind speed is greater than 10 m/s, the wind

Table 5
Spinning reserve of Scenario 1.

Wind speed (m/s)	Spinning reserve requirement (kW)		Spinning reserve ability (kW)		Total fuel cost ($/h)
	USR	DSR	USR	DSR	
4	29,011	631	55,000	46,591	569.7124
5	29,896	1516	55,000	46,897	562.3557
6	31,029	2649	55,000	44,417	554.2965
7	32,336	3956	55,000	44,368	543.4817
8	33,743	5363	55,000	45,000	532.8971
9	35,173	6793	55,000	38,563	522.8442
10	36,553	8173	55,000	39,163	512.3446
11	37,806	9426	55,000	41,021	502.6885

Table 6
Spinning reserve of scenario 2.

Wind speed (m/s)	Spinning reserve requirement (kW)		Spinning reserve ability (kW)		Total fuel cost ($/h)
	USR	DSR	USR	DSR	
4	29,643	1263	55,000	45,336	564.1240
5	31,411	3031	55,000	46,187	551.0162
6	33,678	5298	55,000	44,597	533.7086
7	36,292	7913	55,000	42,451	513.9991
8	39,105	10,725	55,000	37,225	493.5322
9	41,966	13,586	55,000	31,676	472.5265
10	44,725	16,345	55,000	35,118	460.9915
11	47,232	18,852	55,000	32,610	443.6994

Table 7
Spinning reserves of Scenario 3.

Wind speed (m/s)	Spinning reserve requirement (kW)		Spinning reserve ability (kW)		Total fuel cost ($/h)
	USR	DSR	USR	DSR	
4	30,274	1894	55,000	45,000	559.4069
5	32,927	4548	55,000	38,660	539.7448
6	36,327	7948	55,000	44,530	513.6078
7	40,248	11,869	55,000	43,797	484.4793
8	44,468	16,088	55,000	34,860	455.9954
9	48,759	20,379	55,000	29,842	424.9154
10	52,898	24,518	55,000	24,166[a]	398.6180
11	56,659	28,278	55,000[a]	18,396[a]	372.3657

[a] USR or DSR ability is insufficient.

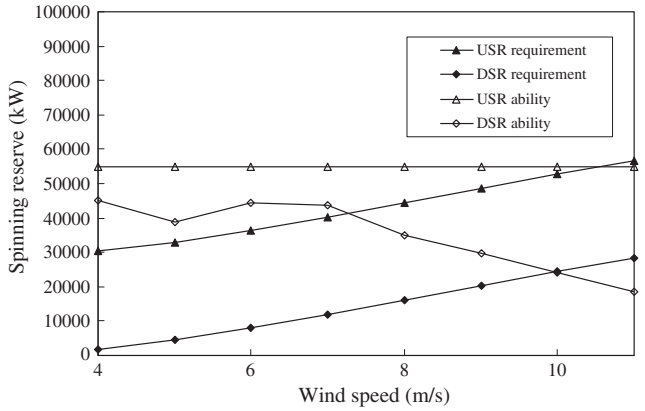

Fig. 4. Spinning reserves vary with wind speeds.

generation is 17% of the power system load. This is greater than 15%, the basic spinning reserve level of the power system. The extra spinning reserve ($r\%$ = 50%), however, makes the power system strong enough to survive under large wind speed variation. In this case, the wind speed changes suddenly from 3 m/s to 10 m/s.

In Scenario 3, the installation capacity of wind generation is 30% of the total power system load. Table 7 shows the computation results. In this case, the high penetration of wind power generation increases generation from the wind turbine generators, decreases generation from the thermal generators, and decrease the down spinning reserve ability of the power system. When the wind speed exceeds 10 m/s, the down spinning ability cannot meet the down spinning reserve requirements. When the wind speed is greater than 11 m/s, the up spinning ability is also insufficient to meet up spinning reserve requirements.

Fig. 4 shows that the spinning reserve varies with the wind speed. This figure shows that as the wind speed increases, the up spinning reserve (USR) requirement also increases. This means

Table 8
Summary of transmission losses and operating costs.

Scenarios	Connected bus		Transmission losses (MW)	Total fuel costs ($/h)
	Bus no.	Voltage (p.u.)		
Without WTGs	–	–	2.233	573.928
Scenario 1	3	1.042	2.1903	436.4135
Scenario 2	8	1.033	2.0549	436.1939
Scenario 3	9	1.024	1.8344	434.9359

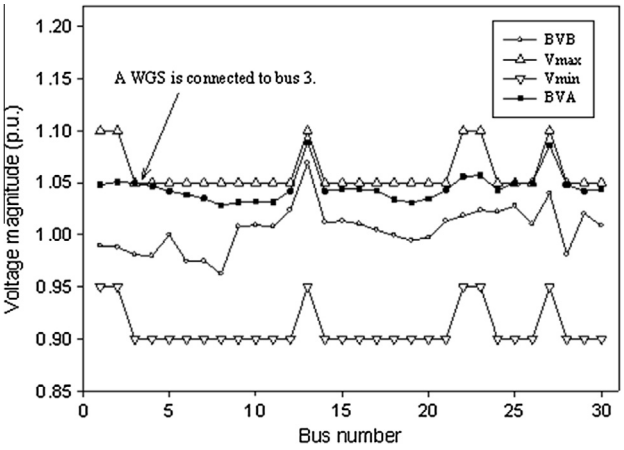

Fig. 5. Voltage distribution of Scenario 1.

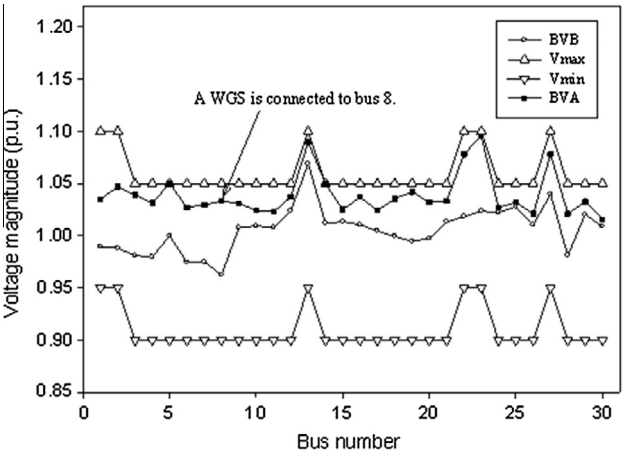

Fig. 6. Voltage distribution of Scenario 2.

power system should supply additional USR to counterbalance the increasing operation risk caused by increasing wind generation. Meanwhile, the down spinning reserve (DSR) requirement also increases when the wind speed increases. Unfortunately, however, the DSR ability decreases as the wind generation increases. This property creates an inherent limit on wind generation installation capacity.

The results above show that, even though wind generation reduces overall operating costs, the increasing up/down spinning reserve requirements caused by wind generation increase power system operating risk.

In conclusion, in a wind-thermal power system, wind generation increases uncertainly power supplies resulted unpredictable power system operation risk. Therefore, it is necessary to reserve

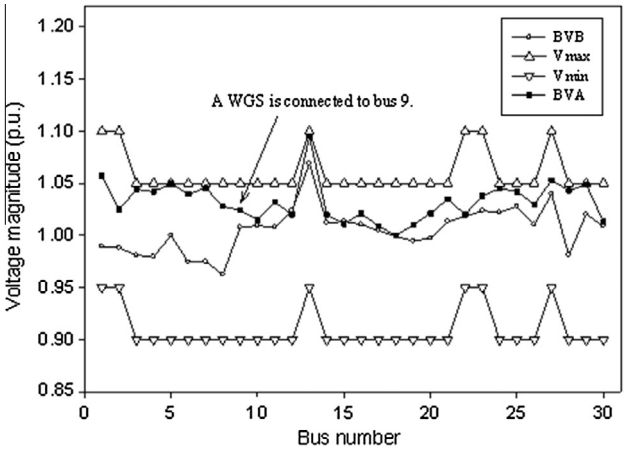

Fig. 7. Voltage distribution of Scenario 3.

Table 9
Transmission loss changes with wind generation locations.

Connected bus			Transmission losses (MW)	Total fuel costs ($/h)
Bus no.	Load (MW)	LSTB		
3	2.4	73	2.1903	436.4135
8	30	58	2.0549	436.1939
9	0	115	1.8344	434.9359

extra up/down spinning reserve ability, as this test demonstrates. The optimal level of up/down spinning reserves remains a problem for future studies to solve.

5.3. Wind generation affects power system voltage

As a wind generation continues to grow, it is becoming more important to investigate the effects of wind generation on power system operation. Bus voltage is one of the most important indices affecting power system operation. This test investigates the effects of wind generation on power system bus voltage distributions. This study conducts three scenarios to estimate the variation of bus voltage distributions when incorporating wind generation into a power system.

Scenario 1: Wind generation is connected to bus 3, a bus close to the generators.
Scenario 2: Wind generation is connected to bus 8, a bus located midway between two neighboring generators.
Scenario 3: Wind generation is connected to bus 9, a bus located at the end of transmission lines.

To satisfy the up/down spinning reserve constraints, the installation capacity of wind generation is set to be 20% of the power system load, the 1st hour wind speed is 3 m/s, and the 2nd hour wind speed is 11 m/s, the power factor of wind generation is assumed to be 1.0. Table 8 summarizes the transmission losses and operating costs of all scenarios.

Fig. 5 shows the voltage distribution of Scenario 1. In this figure, "BVB" is the original bus voltage; "BVA" is the bus voltage after a wind generation system is connected to the power system; "Vmin" is the lower limit of bus voltages; and "Vmax" is the upper limit of bus voltages. In this case, wind generation is connected to bus 3, a bus very close to generator 1, and is located at the source of the transmission system. The voltage distribution profile is smooth, except at buses 13 and 27. However, Scenario 1 has the greatest transmission loss of all scenarios.

Fig. 6 shows the voltage distribution of Scenario 2. In this case, wind generation is connected to bus 8, a bus located at the medium of transmission system. Fig. 6 shows increases in the voltage of all buses, and especially at bus 5, 13, 22, 23, and 27, where the bus voltages are very close to the upper voltage limit.

Fig. 7 shows the voltage distribution of Scenario 3. In this case, wind generation is connected to bus 9, a bus located at the end of transmission lines, and with a low voltage. Fig. 7 shows an increase in the voltage of all buses, and especially at bus 1–8, while the voltage variations at other buses are not obvious. This means that when a wind generation system is connected to the end of a transmission system, it will only affect bus voltage of the buses close to it. Furthermore, this scenario achieves the lowest transmission losses of all cases.

The results above show that it is good to connect wind generation to the end of a transmission line, and especially at a low voltage bus. In this case, wind generation has a good ability to reduce operating costs and avoid low voltage.

5.4. Effects of wind generation on power system transmission losses

The generation of wind generators supplies part of power system load, shares the loading of thermal generators, alters the line flow of transmission lines, and thus changes the transmission losses of a power system. This section evaluates how the location of wind generators affects transmission losses.

Consider a setup in which a wind generation system is connected to buses 3, 8, and 9, respectively. Table 9 lists the load of connected buses, load summation of two levels of neighbor buses (LSTB), transmission losses, and operating costs.

Table 9 shows that when wind generation system is connected to bus 3, a bus near generators. It is located at the source of the transmission system. The effects of wind generation system on reducing transmission losses are not obvious. Thus, this case has the highest transmission loss in Table 9.

When a wind generation system is connected to bus 8, a bus located midway between two neighbor generators, the generation of wind generation reduces the need for generation supplied by thermal generators. This in turn reduces line flows from thermal generators located at the source of the transmission system, effectively reducing transmission losses.

When a wind generation system is connected to bus 9, a bus located at the end of transmission system, bus 9 has no load connected. However, the LSTB of bus 9 is 115 MW, which is greater than all the other cases. This means that bus 9 is located at a large load center. Generation of wind generators inject into power system from the end of the transmission system, reverse line flows on the transmission lines directly connected to bus 9, share part of LSTB, and thus reduce line flow from thermal generators. Hence, this case has the smallest transmission loss of all cases.

The results above show that, for the purpose of reducing transmission losses, a good place to setup a wind generation system is a bus located at the end of transmission system with a large LSTB.

6. Conclusion

This paper proposes an EPSO approach for solving the OPF problem of a wind-thermal power system. The numerical examples in this study evaluate the effects of wind generation on power system OPF. Results show that the EPSO approach is a potential alternative for power system OPF solutions. Test results also show the following:

(1) Transformer tap settings and shunt capacitor capacities affect transmission losses and operating costs.
(2) A wind-thermal power system requires extra up/down spinning reserves. These extra up/down spinning reserves could improve the power system's ability to survive under varying wind generation injection.
(3) The installation capacity of a wind generation system should be limited. The case study results in this study show that when the installation capacity of the wind generation system exceeds 30% of the power system load, the up/down spinning reserves might be insufficient in the high wind speed situations.
(4) The location of the wind generation system affects the voltage distribution and transmission losses. A bus located at the end of the transmission system with large LSTB is a good place to setup a wind generation system.

Acknowledgments

The authors deeply appreciate the support of Taiwan Power Company for providing the system data and test cases. Financial supports under the Grant No. NSC 97-2221-E-159-019 from the National Science Council, Taiwan, ROC are acknowledged.

References

[1] Niknam T, Azizipanah-Abarghooee R, Sedaghati R, Kavousi fard A. An enhanced hybrid particle swarm optimization and simulated annealing for practical economic dispatch. Energy Educ Sci Technol Part A J 2012;30(1):553–64.
[2] Niknam T, Golestaneh F. Enhanced adaptive particle swarm optimization algorithm for dynamic non-convex economic dispatch. IET Gener Trans Distribut 2012;6(5):424–35.
[3] Niknam T, Doagou Mojarrad H, Zeinoddini Meymand H. Non-smooth economic dispatch computation by fuzzy and self adaptive particle swarm optimization. Appl Soft Comput J 2011;11(2):2805–17.
[4] Aghaei J, Niknam T, Azizipanah-Abarghooee R, Arroyo Sanchez JM. Scenario-based dynamic economic emission dispatch considering load and wind power uncertainties. Int J Electr Pow Energy Syst 2013;47:351–67.
[5] AlRashidi MR, El-Hawary ME. Hybrid particle swarm optimization approach for solving the discrete OPF problem considering the valve loading effects. IEEE Trans 2007;PWRS-22(4):2030–8.
[6] Todorovski M, Rajicic D. An initialization procedure in solving optimal power flow by genetic algorithm. IEEE Trans 2006;PWRS-21(2):480–7.
[7] Nakawiro W, Erlich I. A combined ga-ann strategy for solving optimal power flow with voltage security constraint. In: Asia-Pacific power and energy, engineering conference, 2009. p. 1–4.
[8] Ahmadi H, Ghasemi H, Haddadi AM, Lesani H. Two approaches to transient stability-constrained optimal power flow. Int J Electr Pow Energy Syst 2013;47:181–92.
[9] Onate Yumbla PE, Ramirez JM, Coello CA. Optimal power flow subject to security constraints solved with a particle swarm optimizer. IEEE Trans 2008;PWRS-23(1):33–40.
[10] Mo N, Zou ZY, Chan KW, Pong TYG. Transient stability constrained optimal power flow using particle swarm optimisation. IET Gener Trans Distrib 2007;1(3):476–83.
[11] Shanmukha Sundar K, Ravikumar HM. Selection of TCSC location for secured optimal power flow under normal and network contingencies. Int J Electr Pow Energy Syst 2012;34(1):29–37.
[12] Tehzeeb-Ul-Hassan H, Zafar R, Mohsin SA, Lateef O. Reduction in power transmission loss using fully informed particle swarm optimization. Int J Electr Pow Energy Syst 2012;43(1):364–8.
[13] Kumar S, Chaturvedi DK. Optimal power flow solution using fuzzy evolutionary and swarm optimization. Int J Electr Pow Energy Syst 2013;47:416–23.
[14] Niknam T, Narimani MR, Aghaei J, Azizipanah-Abarghooee R. Improved particle swarm optimization for multiobjective optimal power flow considering cost, loss, emission, and voltage stability index. IET Gener Trans Distrib 2012;6(6):515–27.
[15] Mahdad B, Srairi K, Bouktir T. Optimal power flow for large-scale power system with shunt facts using efficient parallel GA. Int J Electr Pow Energy Syst 2010;32(5):507–17.
[16] Sivasubramani S, Swarup KS. Multi-objective harmony search algorithm for optimal power flow problem. Int J Electr Power Energy Syst 2011;33(3):745–52.
[17] Niknam T, Narimani MR, Aghaei J, Tabatabaei S, Nayeripour M. Modified honey bee mating optimization to solve dynamic optimal power flow with considering generator constraints. IET Gener Transm Distrib 2011;5(10):989–1002.
[18] Niknam T, Narimani MR. A new evolutionary optimization algorithm for optimal power flow in a power system involving unified power flow controller. Energy Educ Sci Technol Part A J 2012;29(2):901–12.
[19] Narimani R, Jabbari M. Dynamic optimal power flow using hybrid particle swarm optimization and simulated annealing. Eur Trans Electr Pow 2012. http://dx.doi.org/10.1002/etep.1633.
[20] Niknam T, Narimani MR, Azizipanah R. A new hybrid algorithm for optimal power flow considering prohibited zones and valve point effect. Energy Convers Manage 2012;58(1):197–206.
[21] Niknam T, Narimani MR, Jabbari M, Malekpour AR. A modified shuffle frog leaping algorithm for multi-objective optimal power flow. Energy 2011;36(11):6420–32.
[22] http://www.homerenergy.com/index.asp.
[23] Kennedy J, Eberhart R. Particle swarm optimization. In: Proceeding of IEEE international conference on neural networks, 1995. p. 1942–8.
[24] Fogel DB. Evolutionary computation: toward a new philosophy of machine intelligence. 2nd ed. IEEE Press; 2000.
[25] Lee TY, Chen CL. Wind-PV capacity coordination for a time-of-use rate industrial user. IET Renew Power Gener 2009;3(3):152–67.